Polymer 51 (2010) 6168–6173

Contents lists available at ScienceDirect

Polymer

journal homepage: www.elsevier.com/locate/polymer

# Nitroxide-mediated radical polymerization in nanoreactors: Factors influencing compartmentalization effects on bimolecular termination

Per B. Zetterlund*

*Centre for Advanced Macromolecular Design (CAMD), School of Chemical Engineering, The University of New South Wales, Sydney, NSW 2052, Australia*

ARTICLE INFO

*Article history:*
Received 9 September 2010
Received in revised form
17 October 2010
Accepted 31 October 2010
Available online 4 November 2010

*Keywords:*
Nitroxide-mediated radical polymerization
Miniemulsion polymerization
Compartmentalization

ABSTRACT

Modeling and simulations of nitroxide-mediated radical polymerization (NMP) in dispersed systems have been performed to elucidate what factors dictate the magnitude of the segregation effect on bimolecular termination between propagating radicals generated from alkoxyamine activation. The reduction in termination rate due to segregation cannot be predicted merely based on the average number of propagating radicals per particle ($\bar{n}_p$). This is because the magnitude of the segregation effect is also governed by the distribution of propagating radicals between particles, which is influenced by both the termination ($k_t$) and the deactivation ($k_{deact}$) rate coefficients. The results have implications with regards to improvement of livingness (end-functionality) in NMP by exploitation of particle size, and are expected to apply (qualitatively) to other controlled/living systems based on the persistent radical effect (e.g. atom transfer radical polymerization).



## 1. Introduction

Controlled/living radical polymerization (CLRP) in dispersed systems, where the continuous phase is usually water [1,2], but can also be other media such as supercritical carbon dioxide [3,4], enables synthesis of polymeric nanoparticles of various morphologies comprising well-defined polymer with a number of potential applications. It can be a significant challenge to perform CLRP in a dispersed system (emulsion, miniemulsion, etc.), mainly due to various issues related to colloidal stability, as well as the fact that these systems often contain as many as three different phases (monomer droplets, polymer particles, continuous phase) [1,2]. The intrinsic characteristics associated with CLRP in dispersed systems, e.g. various interface effects [5–11] and compartmentalization [12–15], may dramatically alter the progression of the polymerization as compared to the homogeneous counterpart. It is desirable to develop an understanding of these phenomena such that one is able to influence a CLRP in order to improve the level of control over the molecular weight distribution (MWD) and/or the livingness (end-functionality).

Compartmentalization refers to the physical isolation of reactant species in confined spaces, i.e. the monomer droplets or polymer particles. Compartmentalization effects have been predicted theoretically for nitroxide-mediated radical polymerization (NMP) [13,14,16–22], atom transfer radical polymerization (ATRP) [12,15,20,23,24] and reversible addition-fragmentation chain transfer (RAFT) polymerization [19,20,25–28], and experimental evidence has also been reported for a number of cases [29–32]. In CLRP, compartmentalization may manifest itself in two different ways via the segregation effect and the confined space effect [13]. The segregation effect refers to how two species in different particles cannot undergo chemical reaction, and may thus lead to a reduction in the bimolecular termination rate. This is the fundamental origin of conventional non-living emulsion polymerizations in general yielding higher polymerization rates ($R_p$) and higher molecular weights than bulk/solution polymerizations, and may also lead to improved livingness in CLRP. The confined space effect refers to the rate of reaction between two given species being higher in a small particle than in a large particle. The confined space effect can result in the rate of deactivation between a propagating radical and a deactivator species to increase in CLRP systems that operate according to the persistent radical effect (e.g. NMP and ATRP), which may lead to improved control over the MWD (lower polydispersity).

To date, it remains unclear what factors in CLRP affect the extent of the segregation effect on bimolecular termination of propagating radicals generated from activation of dormant species. To illustrate this, consider the two cases of NMP of styrene at 125 °C mediated by the nitroxides 2,2,6,6-tetramethylpiperidinyl-1-oxy (TEMPO) and 2,2,5-trimethyl-4-phenyl-3-azahexane-3-oxy (TIPNO) in the absence of spontaneous initiation of styrene [33,34] (i.e. the only

* Tel.: +61 2 9385 4331; fax: +61 2 9385 6250.
*E-mail address:* p.zetterlund@unsw.edu.au.

0032-3861/$ – see front matter © 2010 Elsevier Ltd. All rights reserved.
doi:10.1016/j.polymer.2010.10.064

radical source is alkoxyamine activation) [21]. The two systems are identical, except for the fact that the NMP equilibrium constant ($K = k_{act}/k_{deact}$) is approximately a factor of 356 higher for TIPNO than TEMPO, mainly due to the much lower $k_{deact}$ for TIPNO. If one compares the compartmentalized termination rate with that of a bulk system with the same overall propagating radical concentration for $[alkoxyamine]_0 = 0.02$ M at a particle diameter of 50 nm, the segregation effect is close to two orders of magnitude stronger for TIPNO.

In the present work, theoretical investigations have been carried out based on simulations using the previously developed modified Smith–Ewart equations for NMP [13,16] in order to elucidate what factors govern the extent of the segregation effect in NMP in dispersed systems. Ultimately it is hoped that the findings reported herein will aid in future endeavours to exploit particle size and compartmentalization to improve the performance of NMP (as well as other CLRP systems based on the persistent radical effect, e.g. ATRP) in dispersed systems mainly with regards to livingness and thus also the maximum attainable molecular weight.

## 2. Modeling and simulations

### 2.1. Model for NMP in dispersed system

The modeling technique employed to investigate compartmentalization effects in NMP has been described in detail in previous papers and will not be repeated here [13,21,22]. The modified Smith–Ewart equations describe the number fractions of particles $N_i^j$ (particles containing $i$ propagating radicals (P·) and $j$ nitroxide molecules (T·)):

$$\frac{dN_i^j}{dt} = N_A \nu_p k_{act}[PT]\left\{N_{i-1}^{j-1} - N_i^j\right\} + \frac{k_t}{N_A \nu_p}\left\{(i+2)(i+1)N_{i+2}^j - (i)(i-1)N_i^j\right\} + \frac{k_{deact}}{N_A \nu_p}\left\{(i+1)(j+1)N_{i+1}^{j+1} - (i)(j)N_i^j\right\} \quad (1)$$

where $N_A$ is Avogardo's number and $\nu_p$ is the particle volume, and $k_{act}$, $k_t$ and $k_{deact}$ are the rate coefficients for alkoxyamine activation, bimolecular termination, and deactivation, respectively. It is noteworthy that Eq. (1) accounts for compartmentalization of both P· and T·. Eq. (1) is employed to compute the distributions of P· and T· between the particles, and a separate set of equations is then used to calculate the monomer consumption rate and other related quantities [13].

The model corresponds to an ideal miniemulsion polymerization [35], where the system initially comprises monomer droplets that are subsequently converted to polymer particles. The total number of monomer droplets (polymer particles) remains constant (no secondary nucleation or Ostwald ripening). It has been assumed that phase transfer events (e.g. exit and entry of nitroxide) and other species do not occur to make the problem more tractable, although such effects may influence a real system. The equations were implemented and solved using the software VisSim (version 6.0A11, Visual Solutions Inc.) employing numerical integration (Backward Euler integration algorithm).

The base parameter values (rate coefficients) employed in the simulations are listed in Table 1, corresponding to the TEMPO/styrene system at 125 °C (without spontaneous initiation of styrene) with initial monomer and alkoxyamine concentrations of 8.71 (bulk styrene) and 0.02 M, respectively. The initial alkoxyamine was assumed to have the same values of $k_{act}$ and $k_{deact}$ as the polymeric alkoxyamines generated in the polymerization. The simulations were only taken to 1% monomer conversion, and thus conversion-dependence of $k_t$ could be safely neglected [40].

**Table 1**
Base parameter values for TEMPO-mediated radical polymerization of styrene at 125 °C.

| Rate parameter | Value |
|---|---|
| $k_{act}$ (activation) | $1.60 \times 10^{-3}$ s$^{-1}$ [36] |
| $k_{deact}$ (deactivation) | $7.60 \times 10^{7}$ M$^{-1}$ s$^{-1}$ [36,37] |
| $k_p$ (propagation) | $2.32 \times 10^{3}$ M$^{-1}$ s$^{-1}$ [38] |
| $k_t$ (termination)[a] | $1.72 \times 10^{8}$ M$^{-1}$ s$^{-1}$ [39] |

[a] Based on termination rate $= 2k_t[P^\bullet]^2$

Chain-length dependence of rate coefficients (mainly $k_t$ [41]) has not been accounted for.

### 2.2. Quantification of segregation effect

The magnitude of the segregation effect was estimated by comparing the compartmentalized termination rate ($R_t^c$) with the corresponding non-compartmentalized termination rate ($R_t^{nc}$), the latter being the termination rate that would be observed if the organic phase of the dispersed system was instantaneously transformed into a continuous homogeneous bulk phase. The values of $R_t^c$ and $R_t^{nc}$ were computed as follows [13]:

$$R_t^c = \frac{2k_t}{(N_A \nu_p)^2}\sum_i \sum_j i(i-1)N_i^j \quad (2)$$

$$R_t^{nc} = 2k_t[P\cdot]^2 \quad (3)$$

It is important to point out that $R_t^{nc}$ does not correspond to the corresponding bulk system in the sense that it is not the same as what would be obtained if the polymerization was actually carried out in bulk from $t = 0$. It is a hypothetical bulk system where the concentrations are the same as the overall organic phase concentrations at a given conversion (time) in the compartmentalized system in question.

### 2.3. Quantification of confined space effect

The effect of compartmentalization on the deactivation reaction, the confined space effect, was quantified in the same way as the segregation effect on termination, using the following equations [13]:

$$R_{deact}^c = \frac{k_{deact}}{(N_A \nu_p)^2}\sum_i \sum_j ijN_i^j \quad (4)$$

$$R_{deact}^{nc} = k_{deact}[P\cdot][T\cdot] \quad (5)$$

## 3. Results and discussion

The extent of segregation of propagating radicals in a dispersed system increases with decreasing average number of propagating radicals per particle, $\bar{n}_p$:

$$\bar{n}_p = \sum_i \sum_j iN_i^j \quad (6)$$

where $\sum_i \sum_j N_i^j = 1$. However, it is important to distinguish between the extent of segregation and the magnitude of the segregation effect on bimolecular termination. Although intuitively, both quantities would increase with decreasing $\bar{n}_p$, one must remember that $R_t^{nc}$ also decreases with decreasing $\bar{n}_p$ if the

reduction in $\overline{n}_p$ is brought about by a decrease in the overall propagating radical concentration in the organic phase as opposed to by a decrease in particle size.

To clarify this, a series of simulations were performed whereby the segregation effect was quantified by $R_t^c/R_t^{nc}$ as a function of $\overline{n}_p$ for different conditions in terms of particle diameter, $k_t$ and $k_{deact}$. NMP in a dispersed system was thus simulated to 1% monomer conversion employing the base parameter values in Table 1 using the modified Smith–Ewart equations and related equations as outlined in previous publications [13,21]. Subsequently, the quantity $R_t^c/R_t^{nc}$ was calculated from Eqs. (2) and (3). The value of $\overline{n}_p$ in each data series was varied by changing the initial alkoxyamine concentration as listed in Tables S1–S3 (an increase in the initial alkoxyamine concentration leads to an increase in $\overline{n}_p$). The smaller the value of $R_t^c/R_t^{nc}$, the greater is the segregation effect, i.e. the stronger is the reduction in termination rate due to segregation of propagating radicals.

Fig. 1 shows $\log(R_t^c/R_t^{nc})$ for the systems TEMPO/styrene and TIPNO/styrene at 125 °C in the absence of spontaneous initiation of styrene based on previously published simulated data [21], revealing (as described in the Introduction) that the segregation effect is much stronger in the case of TIPNO for reasons that we here set out to clarify.

### 3.1. Effect of particle size

Fig. 2 shows $\log(R_t^c/R_t^{nc})$ plotted vs $\overline{n}_p$ using the base parameter values of Table 1 for three different particle diameters of 50, 70 and 90 nm. Thus, for a fixed value of the particle diameter, $\overline{n}_p$ was varied by changing the initial alkoxyamine concentration, and subsequently $R_t^c/R_t^{nc}$ was calculated at 1% conversion. As $\overline{n}_p$ decreases, the segregation effect becomes stronger, but eventually reaches a constant value that does not change even if $\overline{n}_p$ is reduced further. The maximum magnitude of the segregation effect in these particular cases amounts to a reduction in the termination rate by a factor of approximately 4.3. If $\overline{n}_p$ is sufficiently high, there is no segregation effect, and $R_t^c/R_t^{nc}$ would thus approach unity. In the present simulations, it is not possible to perform simulations under conditions where $R_t^c/R_t^{nc}$ is too close to unity because of a shortcoming of the model related to the maximum number of nitroxide radicals "allowed" per particle [21].

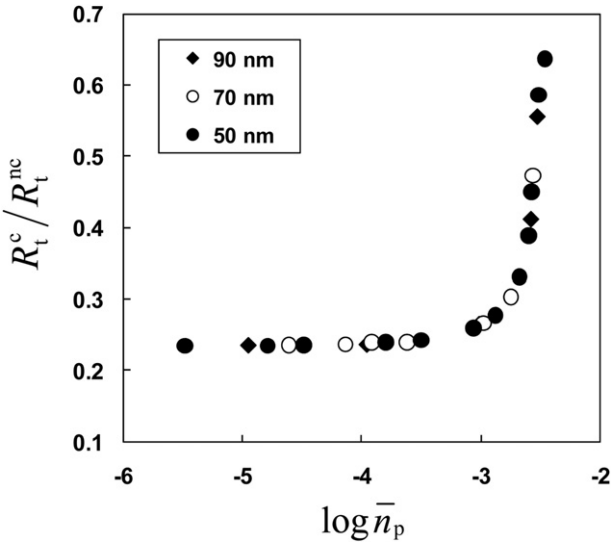


**Fig. 2.** Ratios of "compartmentalized" ($R_t^c$) and "non-compartmentalized" ($R_t^{nc}$) termination rates vs $\log \overline{n}_p$ (propagating radicals per particle) for NMP in a dispersed system with particle diameters as indicated at 1% monomer conversion using rate coefficients from Table 1.

For all three particle diameters, the $R_t^c/R_t^{nc}$ vs $\overline{n}_p$ data points fall on the same master curve. In other words, the magnitude of the segregation effect is independent of the particle size for a fixed value of $\overline{n}_p$. This may seem obvious; however, as we shall see below, the situation is considerably more complex for $R_t^c/R_t^{nc}$ vs $\overline{n}_p$ for different values of $k_t$ and $k_{deact}$.

### 3.2. Effect of termination rate coefficient

Fig. 3 shows plots of $R_t^c/R_t^{nc}$ vs $\overline{n}_p$ for $k_t = 1.72 \times 10^8$ (the literature value for styrene at 125 °C [39]), $1.72 \times 10^7$, and $1.72 \times 10^6$ $M^{-1}\,s^{-1}$. It is immediately apparent that no master curve of $R_t^c/R_t^{nc}$ vs $\overline{n}_p$

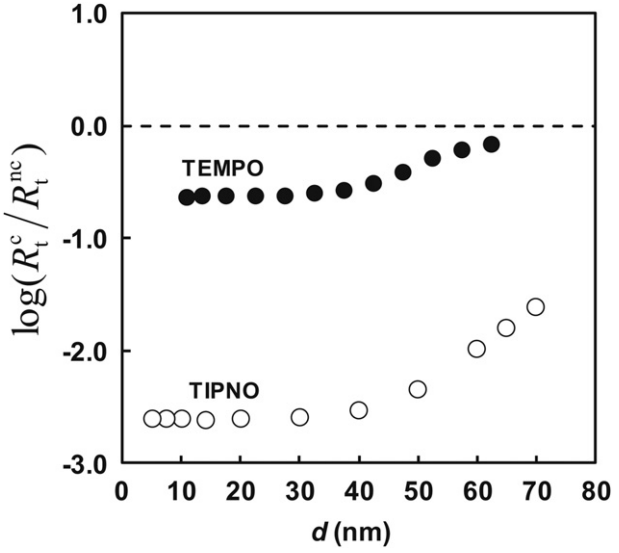


**Fig. 1.** Ratios of "compartmentalized" ($R_t^c$) and "non-compartmentalized" ($R_t^{nc}$) termination rates for TEMPO- (●) and TIPNO- (○) mediated radical polymerization of styrene in dispersed system at different particle diameters ($d$) in the absence of thermal initiation at 125 °C ($[PT]_0 = 0.02$ M) at 1% styrene conversion.

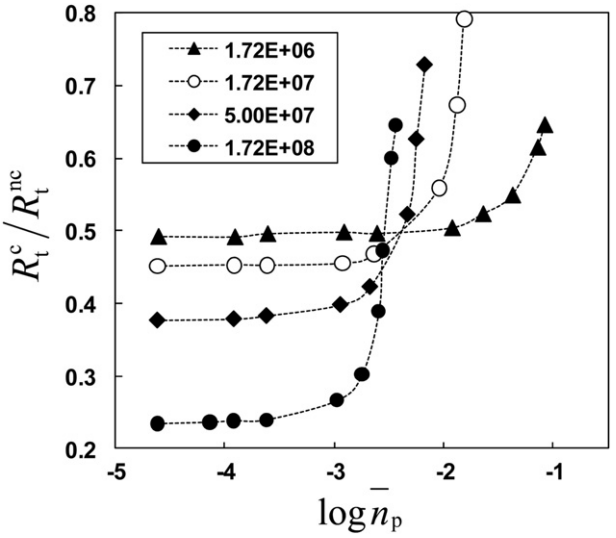


**Fig. 3.** Ratios of "compartmentalized" ($R_t^c$) and "non-compartmentalized" ($R_t^{nc}$) termination rates vs $\log \overline{n}_p$ (propagating radicals per particle) for NMP in a dispersed system for different values of $k_t$ (as indicated in $M^{-1}\,s^{-1}$) at 1% monomer conversion using rate coefficients from Table 1 (except $k_t$). The dotted lines are guides to the eye only.

exists for different values of $k_t$. Thus, at a given value of $\overline{n}_p$, the magnitude of the segregation effect is a function of $k_t$, i.e. the effect of segregation on the termination rate cannot be predicted simply based on $\overline{n}_p$. The higher the value of $k_t$, the stronger is the maximum attainable segregation effect (the constant minimum level of $R_t^c/R_t^{nc}$ reached as $\overline{n}_p$ is reduced). However, the maximum value of $\overline{n}_p$ where segregation effects are still significant appears to decrease with increasing $k_t$. In other words, the "critical" particle size required for segregation effects to be manifested decreases with increasing $k_t$, as previously noted by simulations of conversion-time data [22].

Now, how can it be that even though $\overline{n}_p$ is the same, the extent of the segregation effect depends on the value of $k_t$? To understand this, one must examine the distribution of propagating radicals between particles. It is indeed possible to have two systems with the same $\overline{n}_p$, but different distributions of the propagating radicals between the particles. Information about the distribution of propagating radicals can be gained by examination of the values of $N_i^j$ as computed using Eq. (1).

Table 2 shows the number fractions of various particles $N_i^j$ corresponding to the data in Fig. 3 for $\log \overline{n}_p \approx -2.94$. For termination to occur, a particle must have $i \geq 2$. For all four $k_t$ values, more than 93% of termination events occur in particles of type $N_2^2$ (i.e. $N_2^2$ constitute more than 94% of particles with $i \geq 2$), with a small fraction occurring in $N_2^4$ and a negligible fraction in $N_3^3$. The value of $R_t^c$ is thus approximately proportional to $k_t$ and $N_2^2$ (see Eq. (2)), whereas the value of $R_t^{nc}$ is proportional to $k_t$ and $\overline{n}_p$ (see Eq. (3); $\overline{n}_p$ is proportional to $[P\cdot]$). Therefore, if we wish to compare the magnitude of the segregation effect for two different values of $k_t$, we can write:

$$\frac{\left(R_t^c/R_t^{nc}\right)_{k_{t1}}}{\left(R_t^c/R_t^{nc}\right)_{k_{t2}}} \approx \frac{\left(N_2^2\right)_{k_{t1}}}{\left(N_2^2\right)_{k_{t2}}} \tag{7}$$

where the subscripts $k_{t1}$ and $k_{t2}$ denote different $k_t$ values. Despite $\overline{n}_p$ being the same for all four values of $k_t$, the value of $N_2^2$ decreases with increasing $k_t$ (Table 2). An increase in $k_t$ at the same $\overline{n}_p$ leads to a smaller contribution towards $\overline{n}_p$ from $N_2^2$, whereas the contribution from $N_1^3$ instead increases. Termination can occur in particles of the type $N_2^2$, but not in particles of the type $N_1^3$, and consequently the value of $R_t^c$ decreases with increasing $k_t$. The magnitude of the segregation effect is therefore not only governed by $\overline{n}_p$, but also by the distribution of propagating radicals between the particles, and the latter is affected by $k_t$ even at the same $\overline{n}_p$. A particle of the type $N_2^2$ would be generated when an activation event is followed by a second activation event prior to the first pair of propagating radical and nitroxide having undergone deactivation (i.e. an unlikely event, as reflected in the very low values of $N_2^2$).

### 3.3. Effect of deactivation rate coefficient

Fig. 4 shows plots of $R_t^c/R_t^{nc}$ vs $\overline{n}_p$ for NMP in a dispersed system with particle diameter 70 nm at 1% monomer conversion for $k_{deact} = 7.6 \times 10^6$, $7.6 \times 10^7$ (literature value for styrene/TEMPO at 125 °C [36,37]), and $7.6 \times 10^8\ M^{-1}\ s^{-1}$ using rate coefficients (except $k_{deact}$) from Table 1. Again, it is immediately apparent that no master curve of $R_t^c/R_t^{nc}$ vs $\overline{n}_p$ exists for different values of $k_{deact}$. Consequently, at a given value of $\overline{n}_p$, the magnitude of the segregation effect is also a function of $k_{deact}$. The lower the value of $k_{deact}$, the stronger is the maximum attainable segregation effect, and the larger is the "critical" particle size required for segregation effects to be manifested. The rationale here is essentially the same as for variations in $k_t$ as described above. The extent of the segregation effect on termination is not only dictated by $\overline{n}_p$ but also by the distribution of propagating radicals between the particles, which is influenced by $k_{deact}$.

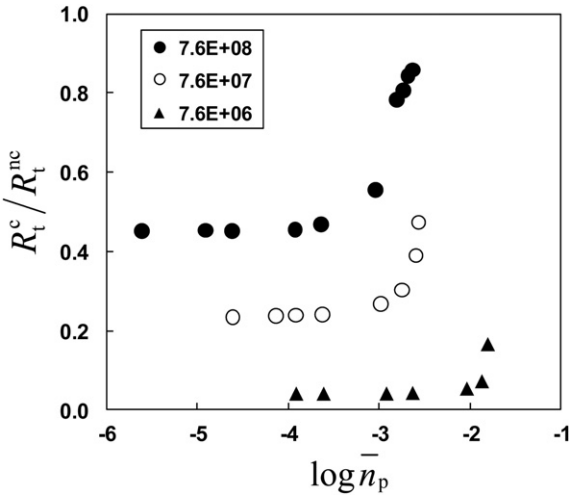


**Fig. 4.** Ratios of "compartmentalized" ($R_t^c$) and "non-compartmentalized" ($R_t^{nc}$) termination rates vs $\log \overline{n}_p$ (propagating radicals per particle) for NMP in a dispersed system for different values of $k_{deact}$ (as indicated in $M^{-1}\ s^{-1}$) at 1% monomer conversion using rate coefficients from Table 1 (except $k_{deact}$).

Table 3 shows the number fractions of various particles $N_i^j$ corresponding to the data in Fig. 4 for $\log \overline{n}_p \approx -3.62$. A decrease in $k_{deact}$ at the same $\overline{n}_p$ leads to a smaller contribution towards $\overline{n}_p$ from $N_2^2$, whereas the contribution from $N_1^1$ increases. Termination can occur in particles of the type $N_2^2$, but not in particles of the type $N_1^1$, and consequently the value of $R_t^c$ decreases with decreasing $k_{deact}$. The very vast majority (>98%) of termination events occur in particles of the type $N_2^2$, and Eq. (7) can thus be applied once again to rationalize the results.

### 3.4. Confined space effect on deactivation

The analysis described above for the effect of segregation on the termination rate was subsequently applied to the confined space effect on deactivation. In this case, we are interested in seeing whether the magnitude of the confined space effect on deactivation can be described by the number-average of nitroxide species per particle ($\overline{n}_T$) only (Eq. (8)), or whether one must consider the distribution of nitroxide between particles.

**Table 2**
Number fractions of particles containing $i$ P· and $j$ T· ($N_i^j$) for NMP in a dispersed system with particle diameter 70 nm at 1% monomer conversion for different values of $k_t$ using rate coefficients (except $k_t$) from Table 1. The data correspond to initial alkoxyamine (PT) concentrations as indicated, giving similar values of $\overline{n}_P$.

| $k_t$ ($M^{-1}\ s^{-1}$) | $[PT]_0$ (M) | $\overline{n}_P$ ($\times 10^3$) | $N_0^0$ | $N_1^1$ ($\times 10^3$) | $N_0^2$ ($\times 10^3$) | $N_2^2$ ($\times 10^7$) | $N_1^3$ ($\times 10^6$) | $N_3^3$ ($\times 10^{12}$) | $N_0^4$ ($\times 10^5$) | $N_2^4$ ($\times 10^{10}$) |
|---|---|---|---|---|---|---|---|---|---|---|
| $1.72 \times 10^6$ | 0.005 | 1.22 | 0.994 | 1.22 | 4.54 | 3.72 | 1.86 | 50.1 | 0.173 | 2.84 |
| $1.72 \times 10^7$ | 0.005 | 1.20 | 0.957 | 1.18 | 41.2 | 3.25 | 17.0 | 38.6 | 15.4 | 24.6 |
| $5 \times 10^7$ | 0.005 | 1.15 | 0.900 | 1.11 | 98.3 | 2.56 | 40.3 | 24.3 | 99.8 | 53.2 |
| $1.72 \times 10^8$ | 0.0058 | 1.19 | 0.759 | 1.08 | 232 | 1.81 | 110 | 11.4 | 755 | 125 |

**Table 3**
Number fractions of particles containing $i$ P· and $j$ T· ($N_i^j$) for NMP in a dispersed system with particle diameter 70 nm at 1% monomer conversion for different values of $k_{deact}$ using rate coefficients (except $k_{deact}$) from Table 1. The data correspond to initial alkoxyamine (PT) concentrations as indicated, giving similar values of $\bar{n}_P$.

| $k_{deact}$ ($M^{-1}$ $s^{-1}$) | $[PT]_0$ (M) | $\bar{n}_P$ ($\times 10^4$) | $N_0^0$ | $N_1^1$ ($\times 10^4$) | $N_0^2$ ($\times 10^3$) | $N_2^2$ ($\times 10^9$) | $N_1^3$ ($\times 10^7$) | $N_3^3$ ($\times 10^{15}$) | $N_0^4$ ($\times 10^6$) | $N_2^4$ ($\times 10^{12}$) |
|---|---|---|---|---|---|---|---|---|---|---|
| $7.6 \times 10^6$ | 0.0001 | 2.44 | 0.992 | 2.44 | 7.44 | 1.22 | 6.09 | 2.06 | 8.58 | 2.81 |
| $7.6 \times 10^7$ | 0.001 | 2.39 | 0.956 | 2.35 | 43.2 | 6.78 | 35.4 | 73.8 | 219 | 69.5 |
| $7.6 \times 10^8$ | 0.01 | 2.32 | 0.918 | 2.26 | 81.1 | 12.5 | 66.5 | 296 | 617 | 194 |

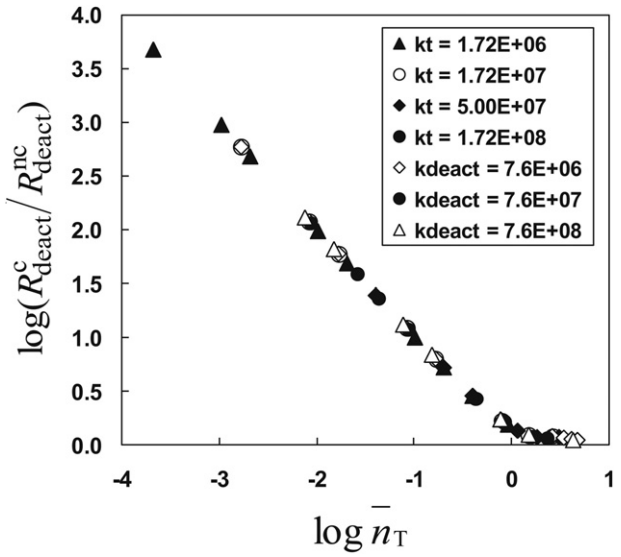


**Fig. 5.** Ratios of "compartmentalized" ($R_t^c$) and "non-compartmentalized" ($R_t^{nc}$) deactivation rates vs log $\bar{n}_T$ (nitroxide radicals per particle) for NMP in a dispersed system at 1% monomer conversion using rate coefficients from Table 1 for different values of $k_t$ and $k_{deact}$ as indicated in $M^{-1}$ $s^{-1}$.

$$\bar{n}_T = \sum_i \sum_j j N_i^j \quad (8)$$

Fig. 5 shows plots of $\log(R_{deact}^c/R_{deact}^{nc})$ vs $\bar{n}_p$ for $k_{deact} = 7.6 \times 10^6$, $7.6 \times 10^7$, and $7.6 \times 10^8$ $M^{-1}$ $s^{-1}$ (with $k_t = 1.72 \times 10^8$ $M^{-1}$ $s^{-1}$) and for $k_t = 1.72 \times 10^6$, $1.72 \times 10^7$, and $1.72 \times 10^8$ $M^{-1}$ $s^{-1}$ (with $k_{deact} = 7.6 \times 10^7$ $M^{-1}$ $s^{-1}$) corresponding to NMP in a dispersed system with particle diameter 70 nm at 1% monomer conversion using rate coefficients (except $k_{deact}$ and $k_t$) from Table 1. All data points fall on the same master curve. It was furthermore confirmed that simulations using different particle diameters of 50 and 90 nm ($k_t = 1.72 \times 10^8$ and $k_{deact} = 7.6 \times 10^7$ $M^{-1}$ $s^{-1}$; data not shown to avoid clutter) also fell on the same master curve as that shown in Fig. 5.

Deactivation can only occur in particles that contain at least one P· and one T·. Examination of the distributions of T· between particles for the different conditions (Table 4) shows particles of the type $N_1^1$ constitute in excess of 98.5% of all particles where $i \geq 1$ and $j \geq 1$, and consequently close to all deactivation events will occur in these particles. Such particles ($N_1^1$) are formed by an activation event occurring in $N_0^0$. Under all conditions simulated, the distribution of T· is essentially the same with regards to the strong dominance of $N_1^1$, and thus the magnitude of the confined space effect is dictated solely by $\bar{n}_T$.

The so called fluctuation effect [14], proposed by Tobita, refers to how fluctuation in the number of T· between different particles can result in an overall deactivation rate that is lower (and thus higher polymerization rate) than that predicted based on all particles containing the same number of T·. The fluctuation effect may be important under certain conditions, but under all conditions examined in this work, such fluctuation effects are insignificant, given that the very vast majority of deactivation events occur in particles of type $N_1^1$.

### 3.5. TEMPO/styrene vs TIPNO/styrene

Finally, let us revisit the simulated data in Fig. 1, which show that the segregation effect on termination is much stronger for TIPNO/styrene than TEMPO/styrene at 125 °C (spontaneous initiation of styrene not included in model). Based on the findings above, these data can now be rationalized based on the value of $k_{deact}$ being a factor of 180 lower in the TIPNO system, which results in a decrease in $N_2^2$, and consequently a lower value of $R_t^c$.

## 4. Conclusions

The nature of the segregation effect on bimolecular termination between propagating radicals generated by alkoxyamine activation in NMP in dispersed systems has been investigated by modeling and simulations employing modified two-dimensional Smith–Ewart equations. It has been shown that the magnitude of the relative reduction in termination rate due to segregation (as compared to a homogeneous system with the same dispersed phase concentration of propagating radicals and nitroxide molecules) cannot be predicted simply from the average number of propagating radicals per particle. The magnitude of the relative reduction in termination rate can be strongly influenced by the distribution of propagating radicals between particles, which is in turn affected by the rate coefficients for termination and deactivation, but unaffected by the particle diameter. The confined space effect on deactivation, on the other hand, can in the investigated systems be predicted solely based on the average number of nitroxide molecules per particle.

The results presented contain important information with regards to how one can potentially exploit segregation effects to improve livingness (end-functionality) in NMP in dispersed systems. For example, the greater the value of the termination rate coefficient, the greater is the maximum possible benefit that can be attained in terms of increased livingness relative to the corresponding homogeneous (bulk/solution) system. The results are expected to apply

**Table 4**
Number fractions of particles containing $i$ P· and $j$ T· ($N_i^j$) for NMP in a dispersed system with particle diameter 70 nm at 1% monomer conversion for different values of $k_{deact}$ using rate coefficients (except $k_{deact}$) from Table 1. The data correspond to initial alkoxyamine (PT) concentrations as indicated, giving similar values of $\bar{n}_T$.

| $k_{deact}$ ($M^{-1}$ $s^{-1}$) | $[PT]_0$ (M) | $\bar{n}_T$ | $N_0^0$ | $N_1^1$ ($\times 10^4$) | $N_0^2$ ($\times 10^3$) | $N_2^2$ ($\times 10^9$) | $N_1^3$ ($\times 10^7$) | $N_3^3$ ($\times 10^{15}$) | $N_0^4$ ($\times 10^6$) | $N_2^4$ ($\times 10^{12}$) |
|---|---|---|---|---|---|---|---|---|---|---|
| $7.6 \times 10^6$ | 0.0005 | 0.077 | 0.961 | 11.8 | 37.6 | 29.4 | 150 | 250 | 225 | 355 |
| $7.6 \times 10^7$ | 0.001 | 0.087 | 0.956 | 2.35 | 43.2 | 6.78 | 35.4 | 73.8 | 219 | 69.5 |
| $7.6 \times 10^8$ | 0.005 | 0.084 | 0.958 | 1.18 | 41.6 | 3.26 | 17.1 | 38.7 | 157 | 24.8 |

(qualitatively) also to other controlled/living systems based on the persistent radical effect, e.g. ATRP.

## Acknowledgement

The author is grateful to the Australian Research Council for a Discovery Grant (DP1093343).

## Appendix. Supplementary data

Supplementary data associated with this article can be found, in the online version, at doi:10.1016/j.polymer.2010.10.064.

## References

[1] Zetterlund PB, Kagawa Y, Okubo M. Chem Rev 2008;108:3747–94.
[2] Cunningham MF. Prog Polym Sci 2008;33:365–98.
[3] Zetterlund PB, Aldabbagh F, Okubo M. J Polym Sci A Polym Chem 2009;47:3711–28.
[4] Thurecht KJ, Howdle SM. Aust J Chem 2009;62:786.
[5] Zetterlund PB, Alam MN, Minami H, Okubo M. Macromol Rapid Commun 2005;26:955–60.
[6] Nakamura T, Zetterlund PB, Okubo M. Macromol Rapid Commun 2006;27:2014–8.
[7] Alam MN, Zetterlund PB, Okubo M. Macromol Chem Phys 2006;207:1732–41.
[8] Zetterlund PB, Nakamura T, Okubo M. Macromolecules 2007;40:8663–72.
[9] Alam MN, Zetterlund PB, Okubo M. J Polym Sci A Polym Chem 2007;45:4995–5004.
[10] Saka Y, Zetterlund PB, Okubo M. Polymer 2007;48:1229–36.
[11] Alam MN, Zetterlund PB, Okubo M. Polymer 2008;49:3428–35.
[12] Kagawa Y, Zetterlund PB, Minami H, Okubo M. Macromol Theory Simul 2006;15:608–13.
[13] Zetterlund PB, Okubo M. Macromolecules 2006;39:8959–67.
[14] Tobita H. Macromol Theory Simul 2007;16:810–23.
[15] Thomson ME, Cunningham MF. Macromolecules; 2010:2772–9.
[16] Butte A, Storti G, Morbidelli M. DECHEMA Monographs, vol. 134; 1998. 497–507.
[17] Charleux B. Macromolecules 2000;33:5358–65.
[18] Zetterlund PB, Okubo M. Macromol Theory Simul 2007;16:221–6.
[19] Tobita H, Yanase F. Macromol Theory Simul 2007;16:476–88.
[20] Tobita H. Macromol Symp 2008;261:36–45.
[21] Zetterlund PB, Okubo M. Macromol Theory Simul 2009;18:277–86.
[22] Zetterlund PB. Macromol Theory Simul 2010;19:11–23.
[23] Zetterlund PB, Kagawa Y, Okubo M. Macromolecules 2009;42:2488–96.
[24] Zetterlund PB. Macromolecules 2010;43(3):1387–95.
[25] Luo Y, Wang R, Yang L, Li B, Zhu S. Macromolecules 2006;39:1328–37.
[26] Tobita H. Macromol Theory Simul 2010;288:16–24.
[27] Tobita H. Macromol Theory Simul 2009;18:108–19.
[28] Tobita H. Macromol Theory Simul 2009;18:120–6.
[29] Wakamatsu J, Kawasaki M, Zetterlund PB, Okubo M. Macromol Rapid Commun 2007;28:2346–53.
[30] Maehata H, Buragina C, Cunningham M, Keoshkerian B. Macromolecules 2007;40:7126–31.
[31] Simms RW, Cunningham MF. Macromolecules 2008;41:5148–55.
[32] Zetterlund PB, Wakamatsu J, Okubo M. Macromolecules 2009;42:6944–52.
[33] Hui AW, Hamielec AE. J Appl Polym Sci 1972;16:749–69.
[34] Khuong KS, Jones WH, Pryor WA. J Am Chem Soc 2005;127:1265–77.
[35] Asua JM. Prog Polym Sci 2002;27:1283.
[36] Goto A, Terauchi T, Fukuda T, Miyamoto T. Macromol Rapid Commun 1997;18:673–81.
[37] Fukuda T, Terauchi T, Goto A, Ohno K, Tsujii Y, Miyamoto T, et al. Macromolecules 1996;29:6393–8.
[38] Buback M, Gilbert RG, Hutchinson RA, Klumperman B, Kuchta FD, Manders BG, et al. Macromol Chem Phys 1995;196:3267–80.
[39] Buback M, Kowollik C, Kurz C, Wahl A. Macromol Chem Phys 2000;201:464–9.
[40] Zetterlund PB, Yamauchi S, Yamada B. Macromol Chem Phys 2004;205:778–85.
[41] Barner-Kowollik C, Russell GT. Prog Polym Sci 2009;34:1211–59.